Neurodevelopmental and transcriptomic effects of CRISPR/Cas9-induced somatic *orco* mutation in honey bees

Zhenqing Chen[a], Ian M. Traniello[#a, b], Seema Rana[#a], Amy Cash-Ahmeda, Alison L. Sankey[a,c], Che Yang[a], Gene E. Robinson[a, b, c]

[a] *Carl R. Woese Institute for Genomic Biology, University of Illinois at Urbana-Champaign, Urbana, IL 61801 (UIUC)*

[b] *Neuroscience Program, UIUC*

[c] *Department of Entomology, UIUC*

[#]These authors contributed equally.

ORCID IDs:

ZC: 0000-0002-9214-9480

IMT 0000-0002-0001-3915

GER: 0000-0003-4828-4068

Neurodevelopmental and transcriptomic effects of CRISPR/Cas9-induced somatic *orco* mutation in honey bees

ABSTRACT

In insects, odorant receptors facilitate olfactory communication and require the functionality of the highly conserved co-receptor gene *orco*. Genome editing studies in a few species of ants and moths have revealed that *orco* can also have a neurodevelopmental function, in addition to its canonical role in adult olfaction, discovered first in *Drosophila melanogaster*. To extend this analysis, we determined whether *orco* mutation also affects the development of the adult brain of the honey bee *Apis mellifera*, an important model system for social behavior and chemical communication. We used CRISPR/Cas9 to knock out *orco* and examine anatomical and molecular consequences. To increase efficiency, we coupled embryonic microinjection with a laboratory egg collection and *in vitro* rearing system. This new workflow advances genomic engineering technologies in honey bees by overcoming restrictions associated with field studies. We used Sanger sequencing to quickly select individuals with complete *orco* knockout for neuroanatomical analyses and later validated and described the mutations with amplicon sequencing. Mutant bees had significantly fewer glomeruli, smaller total glomerular volume, and higher mean glomerulus volume in the antennal lobe compared to wild-type controls. RNA-Sequencing revealed that *orco* knockout also caused differential expression of hundreds of genes in the antenna, including genes related to neural development and genes encoding odorant receptors. The expression of other types of chemoreceptor genes was generally unaffected, reflecting specificity of CRISPR activity in this study. These results suggest that neurodevelopmental effects of *orco* are related to specific insect life histories.

Keywords: Genome editing; Orco; OR; Olfaction; antennal lobe; development; RNA-seq;

INTRODUCTION

Olfaction plays a key role in insect behavior, and insects are able to sense and respond to myriad odorants from their environments. Odorant receptors (ORs) are the largest family of chemosensory proteins in insects (Robertson, 2019) and are expressed in olfactory sensory neurons (OSNs), mostly located in the antennae. Each OSN co-expresses one specific OR together with the highly conserved olfactory coreceptor (ORCO) protein encoded by an *orco* gene. Orco is required for olfaction because it localizes specific ORs to dendritic membranes of OSNs and forms heterodimer ion channels with these ORs to respond to different odors (Sato et al., 2008; Wicher et al., 2008). Insect OSNs with the same OR send projections to specific glomeruli in the antennal lobes, the first olfactory processing center in the brain. Although olfaction in insects and vertebrates shows many commonalities at the anatomical, physiological, and molecular levels, mammalian ORs do not function with a co-receptor (Fleischer, Breer, & Strotmann, 2009).

Recent evidence indicates that *orco* can play different roles in different insect species. In fruit flies (*Drosophila melanogaster*), it has long been known that *orco* is only associated with olfactory sensing in adults and not with antennal lobe development (Chiang, Priya, Ramaswami, VijayRaghavan, & Rodrigues, 2009; Larsson et al., 2004). By contrast, in Indian jumping ants (*Harpegnathos saltator*) and clonal raider ants (*Ooceraea biroi*), CRISPR-induced *orco* mutations did affect antennal lobe development, and also impacted social behavior (Trible et al., 2017; Yan et al., 2017). In the hawkmoth Manduca *sexta*, CRISPR-induced *orco* mutations caused more mild effects on antennal lobe development, and also disrupted olfactory signaling and foraging (Fandino et al., 2019). These results indicate that although the *orco* gene itself is highly conserved, its roles in olfaction vary in different insect species. However, more species need to be studied to look for general patterns across diverse insect lineages.

The western honey bee (*Apis mellifera*) is an important model system for studying olfaction, especially in the context of behaviour. Honey bees live in colonies of tens of thousands of individuals, who coordinate the performance of behavioral tasks primarily through chemical signals (Bortolotti & Costa, 2014; P. G. Ferreira et al., 2013; Winston & Slessor, 1998). Honey bee olfaction has been studied extensively at the neuroanatomical and neurophysiological levels (Galizia et al., 2012) and more recently with genomic tools (Alaux & Robinson, 2007; Guo et al., 2016; Wallberg et al., 2019). A total of 150 ORs have been identified in the most recent assembly of the honey bee genome (Wallberg et al., 2019). So far only one has been functionally characterized, a queen pheromone receptor (Wanner et al., 2007). Honey bees have many more ORs than *Drosophila* (60; Drosophila Odorant Receptor Nomenclature Committee, 2000), but similar numbers to other social insect species (Zhou et al., 2015). The relationship between sociality and OR diversity has led to the hypothesis that OR number is associated with the complexity of a species' chemical ecology and social communication (Robertson, 2019; Yan et al., 2020; Zhou et al., 2012). If this is correct, the *orco* results mentioned above may also be related to differences in life history. We therefore extended this analysis by examining the honey bee. We predicted that the effects of *orco* mutagenesis in honey bees would be similar to what has been observed for ants (Trible et al., 2017; Yan et al., 2017).

Recent applications of genome editing technologies to insects have opened new vistas of discovery for honey bees (Kohno, Suenami, Takeuchi, Sasaki, & Kubo, 2016; Schulte, Theilenberg, Müller-Borg, Gempe, & Beye, 2014). In particular, clustered regularly interspaced short palindromic

repeats/CRISPR-associated protein 9 (CRISPR/Cas9) methodology has recently been made possible in honey bees through a combination of embryonic microinjection, *in vitro* rearing, and artificial diet (Değirmenci et al., 2020; Roth et al., 2019). These studies have generated complete somatic mutants for phenotypic analyses, thus presenting an alternative to the challenges of maintaining honey bee genetic lines in the lab. These tools are also very useful to explore the function of specific genes through targeted mutagenesis, such as *orco*.

We knocked out *orco* in embryonic honey bee workers and performed molecular genotyping to determine the efficacy of the knockout. We then explored downstream effects of *orco* mutation on the adult brain by performing a detailed morphological analysis of antennal lobe glomerular structure. We also measured antennal gene expression to further examine the effects of *orco* mutation on the olfactory system. Our results contribute to an expanded understanding of the role of this important gene.

RESULTS

Degree of somatic *mutagenesis* and knockout efficiency

Our protocols of embryonic injection and *in vitro* rearing with artificial diet were based on published methods (Değirmenci et al., 2020; Roth et al., 2019; Schmehl, Tomé, Mortensen, Martins, & Ellis, 2016), but with some changes as described in Methods. Notably, to facilitate the production of somatic *orco* knock out mutants, we used a laboratory egg collection system that we described previously (Fine et al., 2018; Fig. 1A), which added substantial flexibility to existing honey bee *in vitro* rearing techniques (Fig. 1B-D). This system enables high rates of egg collection independent of weather, which facilitates planning injection and rearing schedules. Injections were performed in the anterior ventral part of 0.5~2 h old embryos; these parameters recently were shown to lead to the strongest effects of genome editing in honey bees (Hu, Zhang, Liao, & Zeng, 2019; Otte et al., 2018)

Honey bee Orco is a seven-transmembrane domain protein. The Cas9 single guide RNA (sgRNA) was designed to target a site in the second exon, 235 bps downstream of the start codon. This cleavage site is in the codon of the 79th amino acid residue, within the second transmembrane domain (Fig. 2A and B). This design was intended to maximize the potential knockout (KO) of *orco* function. Frameshift mutations in this location cause extensive alternation in all downstream domains, and the indels of amino acid residues could potentially disrupt the structure of the transmembrane domain to affect normal function. The sgRNA was *in vitro* transcribed and mixed with purified Cas9 protein to form ribonucleoprotein (RNP) complex solution, which enables the immediate action of Cas9 when injected.

We rapidly genotyped each individual via Sanger sequencing using the Inference of CRISPR Edits (ICE) tool (Hsiau et al., 2018) (https://www.synthego.com/products/bioinformatics/crispr-analysis). This was done to select individuals to be processed for neuroanatomical analysis. This was followed by a slower but more rigorous analysis via Illumina amplicon sequencing for confirmation and more detailed characterization of the induced mutation.

Out of the total 76 CRISPR-injected individuals, we selected 51 for preliminary genotyping via Sanger sequencing. We identified those that appeared to have high knock out efficiency via Sanger sequencing, and selected 25 *orco* CRISPR-injected and 10 buffer-injected control individuals for

neuroanatomical assessment and transcriptomic analysis.

Illumina amplicon sequencing revealed that mutagenesis was highly efficient. Out of the total 76 CRISPR-injected individuals, ~90% generated some degree of mutation, ~50% of which were complete KOs. We also found 15% homozygous biallelic mutants and ~50% heterozygous biallelic mutants (Table 1). For those used for neuroanatomical analysis, percentages were even higher: 72% complete KO and 20% homozygous biallelic mutants (N = 25, Table 2).

The two sequencing methods gave similar results in 40 out of 76 cases. The discrepancies were mostly minor, involving only changes in the adjacent categories listed in Tables 1 and 2, e.g., from multiallelic mutant to heterozygous mutant. For the complete KO samples, the results of Sanger and Illumina amplicon sequencing were highly consistent: 34 individuals showed complete KO in both methods, compared to 36 for Sanger and 40 for Illumina amplicon sequencing.

orco mutation caused extensive neurodevelopmental defects in the honey bee antennal lobe

A total of 25 *orco*-injected and 10 wild type control adult bees aged 0-1 days old were prepared for glomeruli antibody staining and confocal imaging. We selected three control individuals and five KO individuals with superior confocal image quality. The five KO individuals were all confirmed via Illumina amplicon sequencing after neuroanatomical analysis to be complete KOs (two homozygous biallelic and three heterozygous biallelic mutants) (Fig. 2C and D).

orco KO individuals showed extensive antennal lobe compared to controls (Fig. 3A and B and Supplementary Videos 1-4). Total glomerular volume per antennal lobe was significantly lower in *orco* KO individuals compared to controls ($p = 0.0018$, Fig. 3C). *orco* KO individuals also had significantly fewer glomeruli compared to controls ($p = 8.83e\text{-}08$, Fig. 3D). By contrast, average volume per glomerulus was higher in *orco* KO individuals than in controls ($p = 0.00044$, Fig. 3E). In the *orco* KO individuals, there was often a lack of clear boundaries between glomeruli.

orco mutation caused extensive differences in antennal gene expression

In ant *orco* mutants, glomeruli defects were attributed to a loss of antennal OSNs that project to the antennal lobe (Trible et al., 2017; Yan et al., 2017). After observing the antennal lobe defects reported above, we used transcriptomics to explore whether similar consequences also occur in honey bee *orco* mutants. With RNA-Sequencing (RNA-Seq) of antennae from *orco* KO individuals and controls (N = 5 and 5, respectively), we detected 1154 differentially expressed genes (false discovery rate-corrected p-value ≤ 0.05), 433 up-regulated and 721 down-regulated in *orco* KO bees relative to controls (Fig. 4A, and Supplementary Table 2). OR encoding genes were the most affected subfamily of chemosensory genes.

Our transcriptomic analysis included 85 of the 150 genes (including *orco*) predicted to encode OR genes in the honey bee genome (Wallberg et al., 2019). We found different responses to *orco* KO across these ORs: 53 were significantly downregulated in *orco* KO individuals and the other 32 remained unchanged (Fig. 4A, B and Supplementary Table 3). Transcripts of *orco* itself were strongly downregulated in *orco* KO bees compared to controls (log fold change = -4.06).

To examine the possibility of off-target effects of *orco* genome editing, we also used this antennal

transcriptomic analysis to examine the expression of genes encoding other families of chemosensory proteins, including gustatory receptors (GR), ionotropic receptors (IR), odorant binding proteins (OBP), and chemosensory proteins (CP). Out of a total of 38 genes in these categories, we found only two OBP and one IR up-regulated mildly in *orco* KO bees; no GR nor CP genes were differentially expressed (Fig. 4A, B and Supplemental Table 3).

GO analysis detected dozens of terms enriched in both up- and down-regulated genes in *orco* KO bees. For up-regulated genes, there were Biological Process terms mostly associated with various developmental processes such as "structure development," "regulation of cell proliferation," "regulation of stem cell division," "regulation of transcription," and biological rhythms (including "eclosion rhythm") (Fig. 4C). For down-regulated genes, there were Biological Process terms mostly associated with neural activity and normal functions of olfactory sensing, e.g., several terms related to general behavior, cell signals and biological processes in neurons, as well as very specific terms related to synaptic formation and activities. We also saw terms specifically related to OSNs or OSN related tissue, such as "chemosensory behavior," "G-protein coupled signaling pathway," "olfactory receptor activity" and "cilium assembly." We also found GO terms linked to the neurotransmitter acetylcholine, known to be involved in olfaction (Masse, Turner, & Jefferis, 2009), including acetate ester and acetylcholine metabolism genes; they were down-regulated in *orco* mutants. The full lists of GO terms, including Molecular Function and Cellular Components, are included in Supplemental Table 4.

DISCUSSION

We integrated an established *in vitro* rearing system, a new laboratory egg collection system, and CRISPR/Cas9 genome editing technology to develop an efficient method for genetic manipulation in honey bees. By generating somatic mutants, we demonstrated strong effects of *orco* on the development of the honey bee olfactory system, at both the neuroanatomical and molecular levels. These results provide further support for the hypothesis that species differences in *orco* function are related to differences in life history.

We observed strong effects of *orco* KO on antennal lobe structure. These differences involved a reduction in total glomerular volume and the overall number of glomeruli, though each glomerulus was, on average, larger in size. Because the injections occurred in the embryonic stage and analyses were performed early in adulthood, these results likely reflect neurodevelopmental effects of Orco, rather than effects related to adult neural activity or a neurodegenerative response of the adult brain. These findings suggest *orco* is necessary for proper development of the antennal lobe, and thus are more similar to findings in other hymenopterans than in more distantly related fly and moth species. In ants, *orco* has been shown to be necessary for proper antennal lobe development and social behavior (Trible et al., 2017; Yan et al., 2017). By contrast, in fruit flies, *orco* mutation does not seem to impact general antennal lobe anatomy, although it is still required for maintaining OSN axonal integrity (Chiang et al., 2009). Examination of the results for the hawkmoth *Manduca sexta*, suggest that *orco* mutations also affect neurodevelopment, but only a reduction in the size of the pheromone-responsive macroglomeruluar structure in males (Fandino et al., 2019), suggesting a more limited impact similar to fruit flies. These results point to intriguing differences between insect species in *orco* function.

Transcriptomic analysis of the antennae of *orco* KO mutants provided further insight into the

function of *orco* in the honey bee olfactory system. *orco* KO strongly impacted antennal gene expression, with hundreds of genes differentially expressed as a result. We were able to identify 86 out of 150 ORs annotated in the latest assembly of the honey bee genome. This discovery rate is similar to what has been reported or other RNA-Seq analyses of bee antennal tissue (Nie et al., 2018; Zhao et al., 2016). Our results suggest that one group of ORs is dependent on normal Orco function and the other is independent of Orco. It is not possible to determine the fate of the OSNs with orco-dependent ORs in *orco* mutant bees without tissue staining, but we predict that they would either be missing or strongly defective, as in ants (Trible et al., 2017; Yan et al., 2017), due to the reduction of OR gene expression and glomerular counts in antennal lobe.

OSN projections are crucial in separating and defining proto-glomeruli into mature glomeruli in insects, a process in which synaptic partner-matching and connectivity play important roles (Barish & Volkan, 2015). The surviving *orco*-independent neurons were still able to project to the antennal lobes to form glomeruli in *orco* mutants, but these glomeruli were deformed and lacked clearly defined boundaries. Such morphological defects suggest possible failures in proto-glomerulus separation and glomerulus formation. This might be due to a reduction of synaptic structure and activity in the OSNs, as suggested by the GO term analysis. Our results thus extend the findings from ants, which reported significant reduction of antennal OSNs (Trible et al., 2017; Yan et al., 2017); we provide similar results, but for specific ORs.

Our results also have more general implications insect neurodevelopment. *Drosophila* olfactory sensory neurons and antennal lobe neurons are generated by neurogenetic lineages determined by stereotyped genetic programs (Barish & Volkan, 2015; Chai et al., 2019; Chiang et al., 2009; Dobritsa, Van Der Goes Van Naters, Warr, Steinbrecht, & Carlson, 2003; Lai, Awasaki, Ito, & Lee, 2008; Lin et al., 2012; reviewed in Yan et al., 2020), and it is generally thought that insect neurogenesis mostly follows a hardwiring developmental scheme (*NEEDS REF). However, the bee and ant *orco* results challenge this concept, and are more reminiscent of mammalian olfactory systems. Mammalian olfactory systems are highly plastic and dependent on individual ORs for the proper projection of OSNs and glomeruli formation in the olfactory bulb, and defects in these processes could trigger OSN apoptosis (Lodovichi & Belluscio, 2012; Mombaerts, 2006; Nakashima et al., 2013). Exploring the newly discovered plasticity in insects could lead to insights relevant to mammalian systems.

We also observed extreme down-regulation of *orco* transcript levels, which cannot simply be explained by loss or reduction of OSNs. Only 11 OR genes had stronger down-regulation than *orco*, which was down-regulated 16-fold relative to controls. If the reduction of *orco* was only caused by the loss of OSNs, it should have a level of OR down-regulation intermediate to the other genes. In *orco* mutant individuals, the sum of all OR expression levels was 69% of that in the control. This result suggests that there are additional mechanisms other than simple reduction of OSN numbers causing *orco* down-regulation.

The transcriptional regulation of *orco* in *orco* mutants in other insect species has not yet been closely studied, but in mammalian OSNs (which lack an Orco-like protein), ORs have indirect regulatory roles on transcription. Once the first OR initiates expression in a neuron, it elicits a feedback mechanism to maintain its own expression and repress other ORs via a cascade of cellular, biochemical, and epigenetic changes, so that only one OR is expressed per OSN (Dalton, Lyons, & Lomvardas, 2013; T. Ferreira et al., 2014; Lyons et al., 2013). Perhaps Orco also has a

similar feedback mechanism to regulate its own transcription in OSNs, at least in species with neurodevelopmental effects as in honey bees. More generally, extensive upregulation of genes related to development and cell proliferation suggests strong developmental plasticity feedback in the honey bee olfactory system in response to *orco* mutation.

Gene Ontology (GO) functional analysis of the genes differentially expressed as a result of *orco* mutation provide insights into known and perhaps new functions of Orco. Enriched GO terms that reflect known functions of Orco and general olfaction include terms associated with synapse formation, neurotransmitter pathways, neuronal signals, ligand-gated ion channels, G-protein coupled receptor (GPCR) activity, and chemosensory behavior (Chiang et al., 2009; Sato et al., 2008; Wicher, 2018; Wicher et al., 2008) Enriched GO terms that reflect the possibility of additional functions of Orco include "cilium assembly," a surprising term associated with down regulated genes. While Orco is known to play a role in OR localization in the ciliated dendrites of the OSNs in fruit flies (Benton, Sachse, Michnick, & Vosshall, 2006; Larsson et al., 2004), no effects on cellular cilia structure have been reported so far.

This study was facilitated by improvements in laboratory husbandry of honey bees in the laboratory. We integrated a new laboratory egg collection system (Fine et al. 2019) with an established *in vitro* rearing system(Schmehl et al., 2016) and CRISPR/Cas9 genome editing technology to develop a more efficient method for genetic manipulation in honey bees. Our system overcomes a key challenge associated with honey bee research, namely strong dependence on seasonality and weather conditions for egg collection from outside field colonies.

Improvements in rearing efficiency are especially useful because the increasing popularity of CRISPR/Cas9 somatic mutagenesis reduces emphasis on the need to maintain genetic lines for simple mutant analysis; maintenance of genetic lines is especially difficult in honey bees, because they live in large colonies and queens naturally mate with multiple males. However, one important challenge in the use of somatic mutants is to be able to efficiently identify successful mutant genotypes to facilitate phenotypic analysis. Illumina sequencing of amplicons is the current preferred genotyping tool to identify somatic mutations, but the related benchwork and data analysis is time consuming and not always conducive to generating large samples in a timely manner for certain age-related neurobiological and behavioral phenotypes. Some researchers have used amplified fragment length polymorphism (AFLP) or clone-based sequencing of the CRISPR targeted region as an alternative quick analysis tools (Hu et al., 2019; Roth et al., 2019) but AFLP requires expensive fluorescent primers and only reveals changes in sequence length, while clonal sequencing is still laborious. Instead we combined standard Sanger sequencing data and an online ICE tool (Hsiau et al., 2018), thus using basic molecular biology techniques and analysis tools. Although this method is not able to reveal complete allelic information for the *orco* mutants, it performed extremely well in predicting which mutants showed complete KO and thus helped us select KO samples for time-sensitive phenotypic analysis. We then confirmed these results with the more time-consuming and comprehensive Illumina amplicon sequencing. This combination of methods provides the flexibility necessary to perform phenotypic analysis on somatic mutants.

The effects on antennal lobe development observed here and in ants (Trible et al., 2017; Yan et al., 2017) reveal a higher level of neuroplasticity of the insect olfactory system than previously appreciated. Based on studies of *Drosophila*, it is generally thought that the development of the

insect olfactory system is not dependent upon environmental stimuli (Chai, Cruchet, Wigger, & Benton, 2019; Lin, Kao, Yu, Huang, & Lee, 2012) . By contrast, in mammals, environmental stimuli do appear to play a role in the development of the olfactory system because experimental manipulations that affect normal OR function affect OSN projection and glomerular formation and sometimes trigger OSN apoptosis (Trible et al., 2017; Yan et al., 2017). The effects on antennal lobe development in honey bees thus reflect mammalian-like neuroplasticity in the olfactory system.

Variation in *orco* function appears to be related to variation in insect life history. This early conclusion, based only on results from a few species, suggests that the evolutionary history of Orco's role in olfaction is more complex than previously imagined. In *Drosophila,* Orco appears to have only one role (neurophysiology), whereas in bees, ants, and moths it has two (neurophysiology and neurodevelopment). This is puzzling because the Hymenoptera insect order (bees and ants) is more evolutionarily ancient relative to Diptera (*Drosophila*) and Lepidoptera (*Manduca*). However, these three orders exhibit great intraordinal diversification, all dated similarity to the Early Cretaceous (Misof et al., 2014). Such complicated evolution history makes it difficult to give a simple answer about the evolution of *orco* functions. Studies of additional species, aided by new genome editing tools, will help elucidate the evolution and mechanisms of *orco* function.

The present results from bees and those reported for ants (Trible et al., 2017; Yan et al., 2017) suggest that the neurodevelopmental role of *orco* is related to sociality. To it should be possible to thoroughly test this hypothesis by taking advantage of the remarkable diversity of life histories within the Hymenoptera, ranging from solitary through various levels of sociality (Kapheim et al., 2015). Comparative analyses of *orco*, across insect orders and within the Hymenoptera hold promise for elucidating the mechanisms and evolution of this important insect gene.

Material and Methods

CRISPR RNP complex

We expressed the Cas9 protein using the plasmid pET-28b-Cas9-His (#47327, Addgene, Watertown, MA) in Rosetta *E. coli* cells. The His-tagged Cas9 protein was purified with an Ni-NTA Superflow resin column (#30410, Qiagen, Hilden, Germany) and desalted with PD-10 columns (GE Life Sciences). The protein was then eluted in storage buffer (20 mM Tris [pH = 8.0], 200 mM KCl, 10 mM MgCl2, 10% glycerol) at a concentration of 50 µM and stored at -80 °C.

A single guide RNA (sgRNA) targeting *orco* was designed using the CRISPR Guide RNA Design tool in Benchling (http://benchling.com). We used a MiniGene plasmid with the following DNA template containing a T7 promoter and site-specific targeting sequence (in bold and underlined, respectively): **TAATACGACTCACTATAG**GCTGTGCGTGAGAAGAGCA-GTTTCAGAGCTATGCTGGAAACAGCATAGCAAGTTGAAATAAGGCTAGTCCGTTATC AACTTGAAAAAGTGGCACCGAGTCGGTGCTTTTTAAAAGAGACC (Integrated DNA Technologies, Coralville, IA). The plasmid was linearized by BsaI digestion. sgRNA was transcribed *in vitro* with the T7 RiboMAX™ Express Large Scale RNA Production System (#P1320, Promega, Madison, WI) and purified with Monarch RNA Cleanup Kit following

standard protocol in the manual (New England Biolabs, Ipswich, MA).

We performed Cas9 ribonucleoprotein (RNP) assembly following published methods (Burger et al 2016, Fernandez et al 2017) with some changes. Cas9 protein and sgRNA stock solutions were diluted separately and later combined at a 1:2 molar ratio to create 5 µM RNP solution in injection buffer (20 mM HEPES [pH = 7.5], 300 mM KCl, 1 mM $MgCl_2$). After preparation, the RNP solution was checked for good *in vitro* cleavage activity based on a published protocol (Nishimasu et al., 2018). To ensure consistent RNP complex quality across multiple injection batches, a two-step dilution scheme was used. Briefly, the 5 µM solution was split into 6 µL aliquots and stored at -80°C. To prepare for one week of injections, a 6 µL aliquot of 5µM RNP solution was thawed, diluted to 2.5 µM with injection buffer and split into 2-3 µL injection aliquots. The injection aliquots were frozen again at -80 °C and only thawed before injection for single-day use. In such way, the RNP solutions only had two freeze-thaw cycles across different injection batches.

Egg collection and injection

We caged naturally mated queens (Olivarez Honey Bee Inc, Orland, CA) with ~60-100 one-day-old adult worker bees in plastic cages, fed *ad libitum* with 70% pollen paste, water, 30% sugar syrup and honey following our published protocol (Fine et al., 2018). We set up 20 cages for egg collection at 34 °C and 50% relative humidity (RH) in an incubator. To facilitate collection of eggs for injection, Jenter plugs (Karl Jenter GmbH, Frickenhausen, Germany) were fit into pre-drilled holes positioned in the center of cells in the plastic artificial honeycomb in each cage (Fig. 1B and C. After we removed eggs laid overnight, newly laid eggs were collected within a time window of 3-4 h. Eggs were lined up on a circular ring made of beeswax in a Petri dish. The CRISPR RNP complex targeting *orco* was injected with a PLI100 pico injector (Warner Instruments, LLC, Hamden, CT) following published protocols (Hu et al., 2019; Roth et al., 2019; Schulte et al., 2014). For the control group, 1× injection buffer was used to inject embryos from the same batch of embryos on the same day using the same protocol. After injection, a droplet of ~100 µL 16% sulfuric acid was applied to the center of each Petri dish to suppress fungal growth. The Petri dishes were incubated at 35°C in a humid chamber saturated with 16% sulfuric acid solution. Embryos for genotyping were frozen at 80 °C 2-3 days after egg laying.

in vitro ***rearing of injected honey bee larvae***

The injected honey bee embryos were reared *in vitro* with artificial diets following a published protocol (Schmehl et al., 2016) with modifications; feeding was more frequent but the same total amount of diet was given (Fig. 1D and E). The diets were: Diet A, 44.25% royal jelly, 5.3% Glucose, 5.%3 Fructose, 0.9% yeast extract and 44.25% water; Diet B 42.95% royal jelly, 6.4% Glucose, 6.4% Fructose, 1.3% yeast extract and 42.95% water; Diet C 50% royal jelly, 9% Glucose, 9% Fructose, 2.0% yeast extract and 30% water. Three days following injection, embryos were screened for survivors. The hatching larvae were fed with 5 µL Diet A immediately without grafting. The Jenter plugs were then inserted into predrilled holes in a new, sterilized artificial honeycomb and sealed with Axygen® aluminum film (PCR-AS-200, Corning Inc., Corning, NY) to prevent dehydration or contamination. Over the following 7 days, we used the following feeding schedule: Day 1,10µL Diet A; Day 2, 10µL Diet A; Day 3, 20µL Diet B; Day 4 25 µL Diet C; Day 5, 10 µL (am)+25 µL(pm) Diet C; Day 6, 20 µL (am) + 20 µL (pm) Diet C; Day 7 20 µL (am) Diet C. We performed two feedings daily during the time of high consumption to avoid leaving

too much stale food in the cell. The aluminum sealing film was replaced with a microplate lid (#3098, Corning Inc.) after the first 10µL Diet A was administered. Larvae were kept at the same humidity and temperature conditions as the embryos. For pupation, larvae that finished all the diet were transferred to a 75% RH humid chamber at 35 °C; we sandwiched the plates with UV-sterilized Kimwipes (Kimberly-Clark, Irving, TX) to absorb larval defecation before pupation. Plates were vertically arranged to mimic the natural pupal orientation in the beehive. After pupae eclosed, all adults were flash-frozen in liquid nitrogen for genotyping and RNAseq (using wing and antennal tissue respectively); for those selected for neuroanatomical analysis, brains were removed and dissected on wet ice, as described.

Immunofluorescence staining and imaging

We modified an existing protocol (Rössler et al., 2017) for whole-mount brain immuno-fluorescence. All dissections were performed in ice-cold PBS on adult bees within 24 h of eclosion. Briefly, heads were removed, a small window was cut in the frons, and tissue obscuring the brain was removed. The entire head was then prefixed in 4% paraformaldehyde (PFA) in PBS for 1-2 h on wet ice. After prefixation, brains were carefully dissected and fixed overnight in 4% PFA at 4°C. The following day the brain was rinsed in PBS, permeabilized with 0.2% TritonX-100 in PBS (0.2% PBS-Tx), blocked in 2% goat serum in 0.2% PBS-Tx for 1 h at room temperature and incubated in mouse anti-SYNORF1 antibody (1:100 dilution in blocking buffer; #3C11, Developmental Studies Hybridoma Bank, Iowa, USA) for 4-7 days at 4 °C. Brains were then washed in PBS and incubated in CF®488A goat anti-mouse secondary antibody (1:250 dilution in 1% goat serum in PBS;#20011, Biotium, Fremont, CA) with a NucBlue™ (R37605, Invitrogen, Carlsbad, CA) cellular counterstain for 4-14 days at 4 °C. Finally, brains were washed with PBS, serially dehydrated in ethanol and cleared in methyl salicylate.

Whole-mount brain samples were mounted on glass slides using an iSpacer and #1.5 glass coverslip and scanned with a Zeiss LSM880 confocal microscope. The brains regions in the central part of the brain, including the antennal lobes, parts of the mushroom bodies and the suboesophageal ganglion, were scanned with 10X/0.3 objectives to get "overview images" at a lateral resolution of 1.38 µm and a nominal axial resolution of 8 µm. For detailed measurement, higher resolution images of only antennal lobes were obtained with 20X/0.8 objectives at a lateral resolution of 0.42 µm and a nominal axial resolution of 1 µm.

Image processing and analysis

Brain images were deconvoluted by AutoQuant X3 (Media Cybernetics, Rockville, MD). Z-stack projection images were generated by Fiji (Schindelin et al., 2012). High-resolution images of individual antennal lobes were processed with Amira 6.50 (Thermo Fisher Scientific, Waltham, MA). For annotation of glomerular size and volume, the automated hysteresis thresholding method was used to generate the outline of the glomerular regions in the antennal lobes. The outlines were manually edited with the Segmentation Editor tool in Amira to correct flaws in the automated process. Total glomerular volume was calculated with the Material Statistic command. The number of glomeruli were counted manually. Videos of spinning 3D reconstructed brain structures were generated with the Amira animation function to show the changes in antennal lobe morphology. In those videos, the orco *KO* and control samples were shown at the same distance from the virtual camera to allow size comparison . All data met normality assumptions, so we used Student's t-test to compare buffer-injected controls and *orco* KO groups (in R, Version 3.6.1). Raw data and code can be found in the Figshare repository (URL).

Genotyping and sequencing

We utilized both Sanger and Illumina amplicon sequencing to genotype every individual. Sanger sequencing allowed us to rapidly genotype a particular individual before selecting it for neuroanatomical analysis. Illumina amplicon sequencing required more preparation but allowed for more rigorous genotype analysis to confirm the initial genotyping.

Frozen adult antennal or wing tissue or whole embryos were individually homogenized using NucleoType Mouse PCR kit (Thermo Fisher Scientific, Waltham, MA). The unpurified and undiluted lysates were used as templates for PCR and Sanger sequencing. For Illumina amplicon sequencing, libraries were constructed using the protocol outlined in the Illumina 16S metagenomic library preparation (Illumina, San Diego, CA). First stage PCR was performed with *orco*-specific primers along with overhang adapters at the 5' end. Second stage index PCR was performed with a Nextera unique dual (UD) indexing kit (Illumina) and indexed PCR products were purified using Agencourt AMPure XP beads (Beckman Coulter, Brea, CA). The library pool was quantitated via qPCR and sequenced on one MiSeq flowcell for 251 cycles from each end of the fragment using a MiSeq 500-cycle sequencing kit version 2 (Illumina). Fastq files were generated and demultiplexed with the bcl2fastq v2.20 Conversion Software (Illumina). Data were analyzed with CRISPResso2 (Clement et al., 2019) and CrispRVariants package (Lindsay et al., 2016). Raw and processed reads were uploaded to the Gene Expression Omnibus (GEO) under SuperSeries GSE147719 and SubSeries GSE147713. CRISPResso2 code is available in the Figshare repository (URL).

Sanger and Illumina amplicon sequencing enabled us to classify samples into five categories: wild-type (wt), heterozygous monoallelic mutant, multiallelic mutant, heterozygous biallelic mutant, and homozygous biallelic mutant. Mutant samples were also scored by the level of knockout (KO): complete, uncertain, or incomplete. In the Sanger ICE analysis, a KO score was given by the software and we considered a sample with >70% KO score to be a complete KO. Analyzing the results of the Illumina amplicon sequencing, only samples with frameshift or long indel mutant alleles were considered complete KO. Incomplete KOs were samples with either a wt allele or a mutant allele causing only short indels or substitution of amino acid residues in the protein coding sequence. Uncertain KOs were samples in which only one major allele had a frameshift or long indel mutation.

Measuring antennal gene expression

For RNA-Sequencing (RNA-Seq), total RNA was extracted from a single frozen antenna using the PicoPure RNA isolation kit (Thermo Fisher Scientific). Ribosomal RNA was removed using Ribozero HMR Gold kit (Illumina). Sequencing libraries were prepared using the TruSeq Stranded mRNAseq Sample Prep kit (Illumina), quantitated by qPCR and sequenced in one lane for 101 cycles from each end of the fragment on a NovaSeq 6000 system using NovaSeq SP reagent kit (Illumina).

After adapter trimming, fastq reads from 5 *orco* knockout and 5 buffer-injected control individuals were mapped to the most recent honey bee genome assembly (build HAv3.1; Wallberg et al., 2019) using default settings in STAR v2.7.3a (Dobin et al., 2013). Samples were inspected for contamination with common honey bee viruses (Shpigler et al., 2017; Traniello et al., 2020) but only negligible levels were detected. After alignment, we counted numbers of aligned reads using the "featureCounts" command in the Subread v2.0.0 package (Y. Liao, Smyth, & Shi, 2014; Yang

Liao, Smyth, & Shi, 2013). Count data were imported to R and analyzed with edgeR (M.D. Robinson et al., 2010). We filtered out genes that had fewer than one read per million in at least 5 samples, giving us a total of 8868 genes to use for analysis. We performed TMM normalization and used a generalized linear model with treatment group (*orco* KO vs control) as a categorical predictor of gene expression. Differentially expressed genes (DEGs) were calculated using edgeR's quasi-likelihood test functions, and DEGs were subjected to a Benjamini-Hochberg correction for multiple tests with a false discovery rate (FDR) of 0.05 (Supplemental Table 2). To represent the lack of off-target effects in the entire transcriptome (and not just DEGs), we calculated log2 counts per million (CPM). Raw and processed RNA-Seq reads were uploaded to GEO under the SuperSeries GSE147719 and SubSeries GSE147712.

For Gene Ontology analysis, we performed a one-to-one reciprocal best hit BLAST to convert honey bee genes to their *Drosophila* orthologs (Traniello et al., 2020), and these new gene lists were submitted to the GOrilla database for GO enrichment and REViGO for visualization in semantic space (Eden, Navon, Steinfeld, Lipson, & Yakhini, 2009; Supek et al, 2011). All R code is available in the Figshare repository (URL: ZZ).

Acknowledgements

We thank P. Hanke for assistance with Cas9 protein preparation, L. Licitis and M. Seyller for assistance with the bees, A. Hamilton, K. Torres, N. Beach and J. Fine for support and suggestions on *in vitro* rearing, and members of the Robinson lab for helpful dicussion. The work is funded by NSF NeuroNex grant NSF-DBI 1707221(PI: Y. Ben-Shahar) and DARPA grant XXXXX (PI: GER).

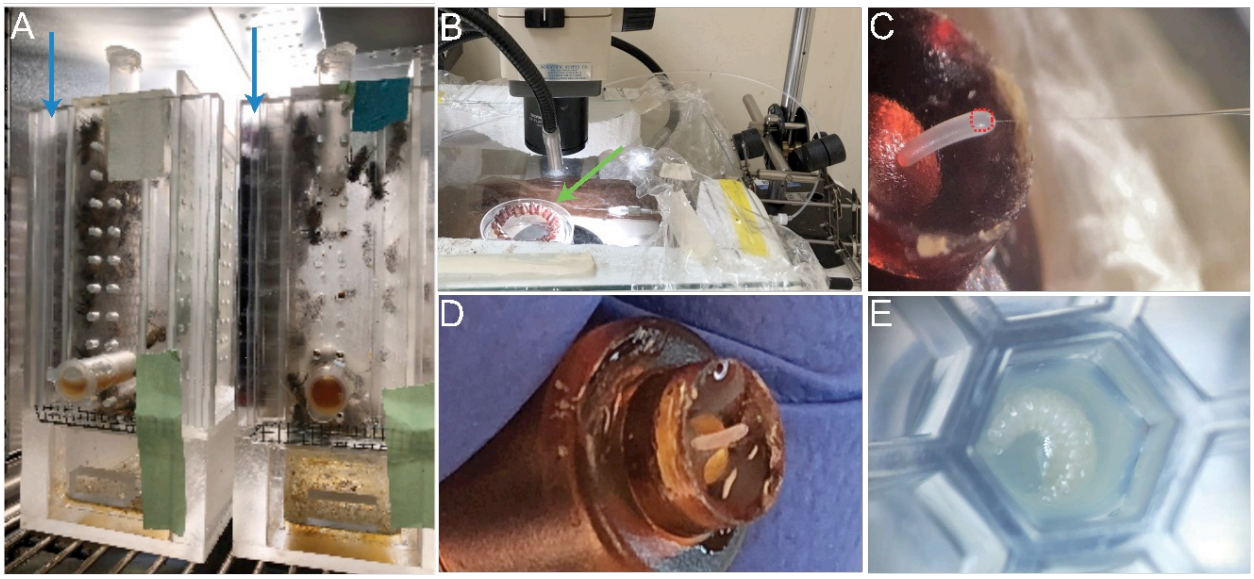

Figure 1. Experimental workflow including setup of egg collection, injection, and *in vitro* rearing.

A) Honey bee queens were caged with 50-100 adult workers in plastic cages with clear plastic artificial honeycomb modified to house Jenter plugs (blue arrows).

B) Brown Jenter plugs with eggs were aligned along a ring of white beeswax in a Petri dish (green arrow) inside a humid chamber built with glass and Styrofoam blocks.

C) Reagent was injected into the anterior ventral part of the embryo (red dashed circle). The orientation of the Jenter plug was adjusted manually to achieve the best injection angle for each embryo.

D) Three days post-injection, embryos were given a small amount of diet around the time of hatching.

E) Honey bee larva floating on a pool of artificial diet during *in vitro* rearing.

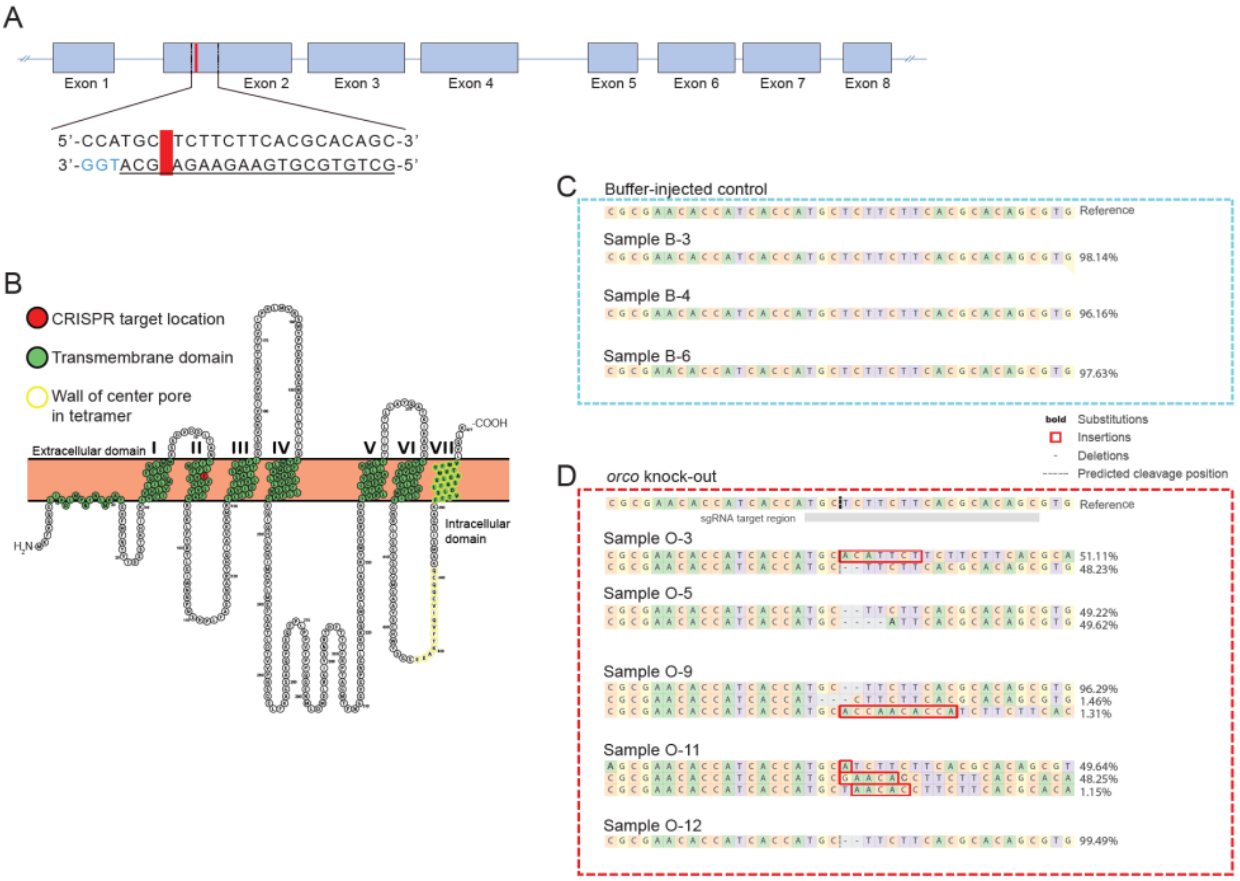

Figure 2. CRISPR/Cas9 design strategy and detection of somatic *orco* mutations.

A) The genomic locus of the honey bee *orco* gene. The target of the CRISPR reagent is in Exon 2; cleavage site (red), sgRNA target sequence (underlined) and PAM sequence (blue) are shown.

B) The predicted protein structure of Orco. The protein has seven transmembrane domains numbered I to VII. The CRISPR target is in the second transmembrane domain, with the codon positioned at the cut site shown in red. Other amino acid residues are colored according to their sequence homology to important structural domains in published Cryo-EM data (Butterwick et al., 2018). Scheme prepared using the Protter web tool (Omasits et al., 2014)).

C) *orco* allelic composition from the three control individuals used in brain neuroanatomical analysis.

D) *orco* allele composition from the five *orco* mutant individuals used in the brain neuroanatomical analysis. Only differences in the region around the sgRNA target are shown. For simplicity, we only present the 40-base window around the cut site, which was used for analysis with CRISPResso2.

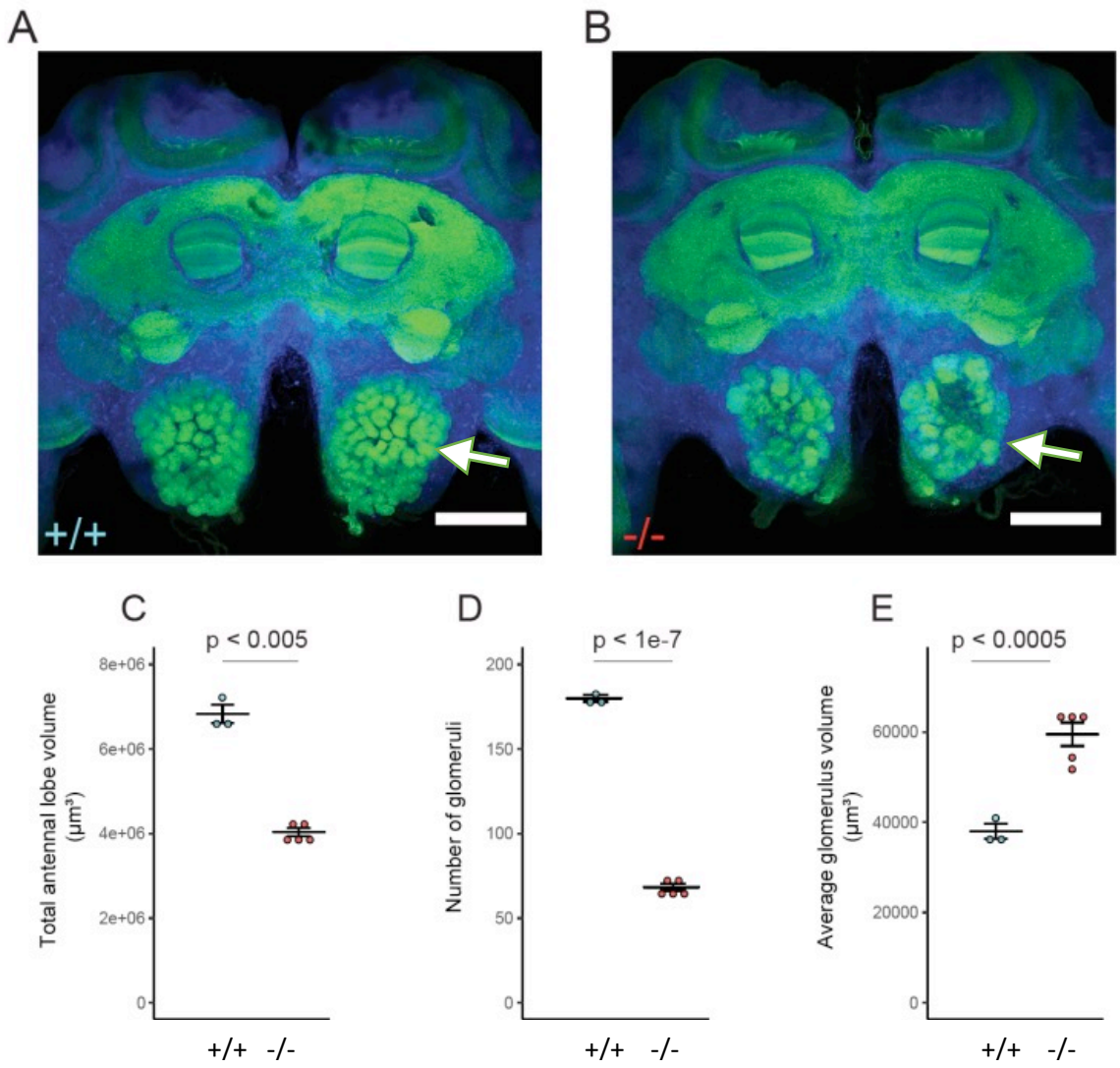

Figure 3. *orco* mutants have neurodevelopmental defects in the antennal lobes.
A and B) Stacked confocal images of honey bee brain samples stained with anti-Syn antibody (green) and counterstained with nuclear label DAPI (blue). Only the central brain regions (tissue excluding optic lobes) were imaged. A control brain is shown in (A) and an *orco* KO brain in (B). Arrows point to antennal lobes. Objective:10x. Scale bar: 200 µm.
C) Effect of *orco* KO on antennal lobe volume. +/+ = wild type control (N = 3; -/- = *orco* KO (N = 5).
D) Effect of *orco* KO on antennal lobe glomerular number. Notation as in Figure 3C.
E) Effect of *orco* KO on antennal lobe glomerular volume. Notation as in Figure 3C.

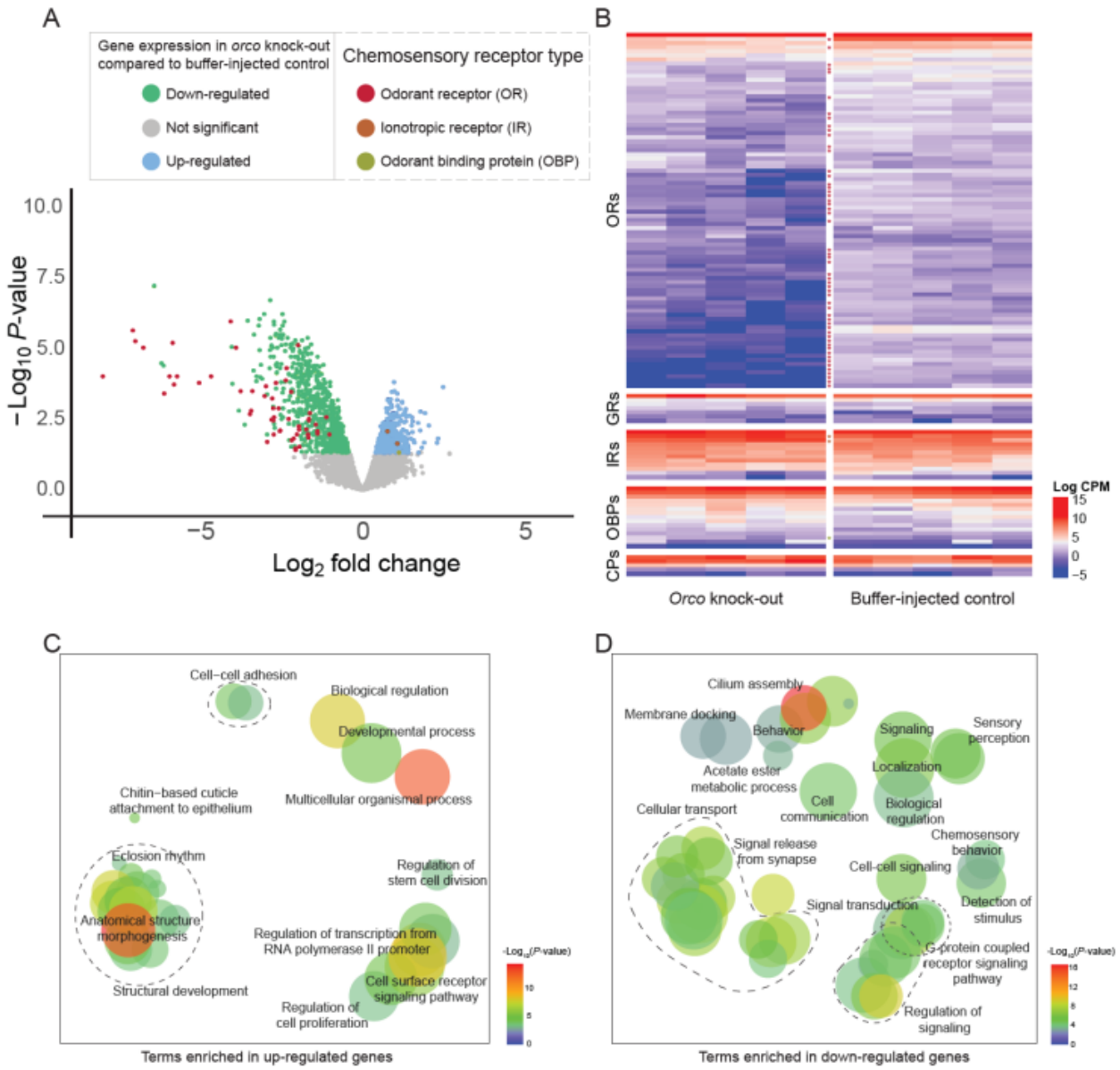

Figure 4. *orco* mutants show extensive differences in antennal gene expression.
A) Volcano plot showing 721 down-regulated (green) and 433 up-regulated (blue) genes in *orco*-KO individuals relative to controls (False discovery rate-corrected p-value ≤ 0.05).
B) Heatmap of gene expression (log counts-per-million values) for all chemosensory genes identified by transcriptomic profiling, including odorant receptors (ORs), gustatory receptors (GRs), ionotropic receptors (IRs), odorant binding proteins (OBPs), and chemosensory proteins (CPs). The majority of the chemosensory genes found to be differentially expressed were also ORs (red asterisk), with minimal evidence for off-target effects among other chemosensory genes. Asterisks denote genes significantly differentially expressed; asterisk color corresponds to chemosensory receptor type, shown in the Fig. 4A legend.
C and D) Biological Processes identified by Gene Ontology enrichment analysis in up-regulated (C) and down-regulated (D) genes. More similar terms are more closely positioned in semantic space, and circle size is inversely correlated with specificity of GO term (with smaller circles

603 representing more specific terms in the GO hierarchy), and significance related to gene list
604 enrichment score for a particular term. Full lists containing all significantly enriched Biological
605 Process, Molecular Function and Cellular Component GO terms are in Supplementary Table 4.
606

607 Table 1. Genotypes of the *orco* injected individuals analyzed by Illumina amplicon sequencing;
608 these individuals werevused to refine the *orco* injection and rearing protocols.

Categories of mutation	**Number per category**	**Complete KO**	**Uncertain KO**	**Incomplete KO**
Homozygous biallelic mutant	7 (13.7%)	7 (13.7%)	0	0
Heterozygous biallelic mutant	29 (56.9%)	13 (25.5%)	10 (19.6%)	6 (11.8%)
Multiallelic mutant	8 (15.7%)	2 (3.92%)	5 (9.81%)	
Heterozygous monoallelic mutant	1 (1.3%)	0%	0	1 (1.3%)
WT or WT like	6 (11.8%)			
Total	51	32 (62.7%)	15 (29.4%)	7 (13.7%)

609

610 Table 2. Genotypes of the *orco* injected individuals analyzed by amplicon sequencing from
611 which we selected individuals for brain neuroanatomical analysis.

Categories of mutation	**Number per category**	**Complete KO**	**Uncertain KO**	**Incomplete KO**
Homozygous biallelic mutant	5 (20%)	5 (20%)	0	0
Heterozygous biallelic mutant	13 (52%)	12 (48%)	1 (4%)	0
Multi-allelic mutant	5 (20%)	1 (4%)	3 (12%)	1 (4%)
WT or WT like	2 (8%)			
Total	25	18 (72%)	4 (16%)	1 (4%)

612
613 Complete KO : only frameshift mutations or indel > 12bps in all alleles
614 Uncertain KO: frameshift mutations or indel only in one major allele
615 Incomplete KO, (only short aa deletion/insertion/substitution in major alleles, or large percentage
616 of wt allele in mutant samples. Wt samples were not counted in this category.
617 Only changes in or close to cleavage sites are considered in genotyping.
618
619
620
621

References

Abel, R., Rybak, J., & Menzel, R. (2001). Structure and response patterns of olfactory interneurons in the honeybee, Apis mellifera. *Journal of Comparative Neurology*. https://doi.org/10.1002/cne.1289

Alaux, C., & Robinson, G. E. (2007). Alarm pheromone induces immediate-early gene expression and slow behavioral response in honey bees. *Journal of Chemical Ecology*, *33*(7), 1346–1350. https://doi.org/10.1007/s10886-007-9301-6

Barish, S., & Volkan, P. C. (2015, November). Mechanisms of olfactory receptor neuron specification in Drosophila. *Wiley Interdisciplinary Reviews: Developmental Biology*. John Wiley & Sons, Inc. https://doi.org/10.1002/wdev.197

Benton, R., Sachse, S., Michnick, S. W., & Vosshall, L. B. (2006). Atypical membrane topology and heteromeric function of Drosophila odorant receptors in vivo. *PLoS Biology*, *4*(2), 240–257. https://doi.org/10.1371/journal.pbio.0040020

Bortolotti, L., & Costa, C. (2014). Chemical Communication in the Honey Bee Society. *Neurobiology of Chemical Communication*, 147–210. https://doi.org/doi:10.1201/b16511-6

Butterwick, J. A., del Mármol, J., Kim, K. H., Kahlson, M. A., Rogow, J. A., Walz, T., & Ruta, V. (2018). Cryo-EM structure of the insect olfactory receptor Orco. *Nature*, *560*(7719), 447–452. https://doi.org/10.1038/s41586-018-0420-8

Chai, P. C., Cruchet, S., Wigger, L., & Benton, R. (2019). Sensory neuron lineage mapping and manipulation in the Drosophila olfactory system. *Nature Communications*, *10*(1). https://doi.org/10.1038/s41467-019-08345-4

Chiang, A., Priya, R., Ramaswami, M., VijayRaghavan, K., & Rodrigues, V. (2009). Neuronal activity and Wnt signaling act through Gsk3-β to regulate axonal integrity in mature Drosophila olfactory sensory neurons. *Development*, *136*(8), 1273–1282. https://doi.org/10.1242/dev.031377

Clement, K., Rees, H., Canver, M. C., Gehrke, J. M., Farouni, R., Hsu, J. Y., … Pinello, L. (2019, March). CRISPResso2 provides accurate and rapid genome editing sequence analysis. *Nature Biotechnology*. Nature Publishing Group. https://doi.org/10.1038/s41587-019-0032-3

Dalton, R. P., Lyons, D. B., & Lomvardas, S. (2013). Co-opting the unfolded protein response to elicit olfactory receptor feedback. *Cell*. https://doi.org/10.1016/j.cell.2013.09.033

Değirmenci, L., Geiger, D., Rogé Ferreira, F., Keller, A., Krischke, B., Beye, M., … Scheiner, R. (2020). CRISPR/Cas9 mediated mutations as a new tool for studying taste in honeybees. *BioRxiv Genetics*, 2020.03.26.009696. https://doi.org/10.1101/2020.03.26.009696

Dobin, A., Davis, C. A., Schlesinger, F., Drenkow, J., Zaleski, C., Jha, S., … Gingeras, T. R. (2013). STAR: ultrafast universal RNA-seq aligner. *Bioinformatics*, *29*(1), 15–21. https://doi.org/10.1093/bioinformatics/bts635

Dobritsa, A. A., Van Der Goes Van Naters, W., Warr, C. G., Steinbrecht, R. A., & Carlson, J. R. (2003). Integrating the molecular and cellular basis of odor coding in the Drosophila antenna. *Neuron*. https://doi.org/10.1016/S0896-6273(03)00094-1

Eden, E., Navon, R., Steinfeld, I., Lipson, D., & Yakhini, Z. (2009). GOrilla: a tool for discovery and visualization of enriched GO terms in ranked gene lists. *BMC Bioinformatics*, *10*(1), 48. https://doi.org/10.1186/1471-2105-10-48

Fandino, R. A., Haverkamp, A., Bisch-Knaden, S., Zhang, J., Bucks, S., Nguyen, T. A. T., … Große-Wilde, E. (2019). Mutagenesis of odorant coreceptor Orco fully disrupts foraging but

not oviposition behaviors in the hawkmoth Manduca sexta. *Proceedings of the National Academy of Sciences of the United States of America*, *116*(31), 15677–15685. https://doi.org/10.1073/pnas.1902089116

Ferreira, P. G., Patalano, S., Chauhan, R., Ffrench-Constant, R., Gabaldon, T., Guigo, R., & Sumner, S. (2013). Transcriptome analyses of primitively eusocial wasps reveal novel insights into the evolution of sociality and the origin of alternative phenotypes. *Genome Biology*, *14*(2), 1–15.

Ferreira, T., Wilson, S. R., Choi, Y. G., Risso, D., Dudoit, S., Speed, T. P., & Ngai, J. (2014). Silencing of odorant receptor genes by G Protein βγ signaling ensures the expression of one odorant receptor per olfactory sensory neuron. *Neuron*. https://doi.org/10.1016/j.neuron.2014.01.001

Fine, J. D., Shpigler, H. Y., Ray, A. M., Beach, N. J., Sankey, A. L., Cash-Ahmed, A., … Robinson, G. E. (2018). Quantifying the effects of pollen nutrition on honey bee queen egg laying with a new laboratory system. *PLOS ONE*, *13*(9), e0203444. https://doi.org/10.1371/journal.pone.0203444

Fleischer, J., Breer, H., & Strotmann, J. (2009). Mammalian olfactory receptors. *Frontiers in Cellular Neuroscience*. https://doi.org/10.3389/neuro.03.009.2009

Guo, Y., Wang, Z., Li, Y., Wei, G., Yuan, J., Sun, Y., … Chen, R. (2016). Lateralization of gene expression in the honeybee brain during olfactory learning. *Scientific Reports*. https://doi.org/10.1038/srep34727

Hsiau, T., Conant, D., Maures, T., Waite, K., Yang, J., Kelso, R., … Stoner, R. (2018). Inference of CRISPR Edits from Sanger Trace Data. *BioRxiv The Preprint Server Biology*. https://doi.org/10.1101/251082

Hu, X. F., Zhang, B., Liao, C. H., & Zeng, Z. J. (2019). High-Efficiency CRISPR/Cas9-Mediated Gene Editing in Honeybee (Apis mellifera) Embryos. *G3 (Bethesda, Md.)*, *9*(5), 1759–1766. https://doi.org/10.1534/g3.119.400130

Kapheim, K. M., Pan, H., Li, C., Salzberg, S. L., Puiu, D., Magoc, T., … Zhang, G. (2015). Genomic signatures of evolutionary transitions from solitary to group living. *Science*, *348*(6239), 1139–1143. https://doi.org/10.1126/science.aaa4788

Kohno, H., Suenami, S., Takeuchi, H., Sasaki, T., & Kubo, T. (2016). Production of Knockout Mutants by CRISPR/Cas9 in the European Honeybee, Apis mellifera L. *Zoological Science*, *33*(5), 505–512. https://doi.org/10.2108/zs160043

Lai, S. L., Awasaki, T., Ito, K., & Lee, T. (2008). Clonal analysis of Drosophila antennal lobe neurons: Diverse neuronal architectures in the lateral neuroblast lineage. *Development*, *135*(17), 2883–2893. https://doi.org/10.1242/dev.024380

Larsson, M. C., Domingos, A. I., Jones, W. D., Chiappe, M. E., Amrein, H., & Vosshall, L. B. (2004). Or83b encodes a broadly expressed odorant receptor essential for Drosophila olfaction. *Neuron*, *43*(5), 703–714. https://doi.org/10.1016/j.neuron.2004.08.019

Liao, Y., Smyth, G. K., & Shi, W. (2014). featureCounts: an efficient general purpose program for assigning sequence reads to genomic features. *Bioinformatics*, *30*(7), 923–930. https://doi.org/10.1093/bioinformatics/btt656

Liao, Yang, Smyth, G. K., & Shi, W. (2013). The Subread aligner: fast, accurate and scalable read mapping by seed-and-vote. *Nucleic Acids Research*, *41*(10), e108–e108. https://doi.org/10.1093/nar/gkt214

Lin, S., Kao, C. F., Yu, H. H., Huang, Y., & Lee, T. (2012). Lineage Analysis of Drosophila Lateral Antennal Lobe Neurons Reveals Notch-Dependent Binary Temporal Fate Decisions.

PLoS Biology. https://doi.org/10.1371/journal.pbio.1001425
Lindsay, H., Burger, A., Biyong, B., Felker, A., Hess, C., Zaugg, J., … Robinson, M. D. (2016). CrispRVariants charts the mutation spectrum of genome engineering experiments. *Nature Biotechnology*. https://doi.org/10.1038/nbt.3628
Lodovichi, C., & Belluscio, L. (2012). Odorant Receptors in the Formation of the Olfactory Bulb Circuitry Organization of the Mammalian Olfactory System. *PHYSIOLOGY*, *27*, 200–212. https://doi.org/10.1152/physiol.00015.2012
Lyons, D. B., Allen, W. E., Goh, T., Tsai, L., Barnea, G., & Lomvardas, S. (2013). XAn epigenetic trap stabilizes singular olfactory receptor expression. *Cell*. https://doi.org/10.1016/j.cell.2013.06.039
Magklara, A., & Lomvardas, S. (2013, September 1). Stochastic gene expression in mammals: Lessons from olfaction. *Trends in Cell Biology*. Elsevier. https://doi.org/10.1016/j.tcb.2013.04.005
Masse, N. Y., Turner, G. C., & Jefferis, G. S. X. E. (2009, August 25). Olfactory Information Processing in Drosophila. *Current Biology*. Elsevier. https://doi.org/10.1016/j.cub.2009.06.026
Menzel, R., Hammer, M., Müller, U., & Rosenboom, H. (1996). Behavioral, neural and cellular components underlying olfactory learning in the honeybee. In *Journal of Physiology Paris*. https://doi.org/10.1016/S0928-4257(97)87928-4
Menzel, Randolf. (2012). The honeybee as a model for understanding the basis of cognition. *Nature Reviews Neuroscience*, *13*(11), 758–768. https://doi.org/10.1038/nrn3357
Menzel, Randolf, Galizia, G., Müller, D., & Szyszka, P. (2005). Odor coding in projection neurons of the honeybee brain. In *Chemical Senses*. https://doi.org/10.1093/chemse/bjh234
Misof, B., Liu, S., Meusemann, K., Peters, R. S., Donath, A., Mayer, C., … Zhou, X. (2014). Phylogenomics resolves the timing and pattern of insect evolution. *Science (New York, N.Y.)*, *346*(6210), 763–767. https://doi.org/10.1126/science.1257570
Mombaerts, P. (2006). Axonal Wiring in the Mouse Olfactory System. *Annual Review of Cell and Developmental Biology*. https://doi.org/10.1146/annurev.cellbio.21.012804.093915
Nakashima, A., Takeuchi, H., Imai, T., Saito, H., Kiyonari, H., Abe, T., … Sakano, H. (2013). Agonist-independent GPCR activity regulates anterior-posterior targeting of olfactory sensory neurons. *Cell*, *154*(6). https://doi.org/10.1016/j.cell.2013.08.033
Nie, H., Xu, S., Xie, C., Geng, H., Zhao, Y., Li, J., … Su, S. (2018). Comparative transcriptome analysis of Apis mellifera antennae of workers performing different tasks. *Molecular Genetics and Genomics*, *293*(1), 237–248. https://doi.org/10.1007/s00438-017-1382-5
Nishimasu, H., Shi, X., Ishiguro, S., Gao, L., Hirano, S., Okazaki, S., … Nureki, O. (2018). Engineered CRISPR-Cas9 nuclease with expanded targeting space. *Science (New York, N.Y.)*, *361*(6408), 1259–1262. https://doi.org/10.1126/science.aas9129
Omasits, U., Ahrens, C. H., Müller, S., & Wollscheid, B. (2014). Protter: Interactive protein feature visualization and integration with experimental proteomic data. *Bioinformatics*, *30*(6), 884–886. https://doi.org/10.1093/bioinformatics/btt607
Otte, M., Netschitailo, O., Kaftanoglu, O., Wang, Y., Page, R. E., & Beye, M. (2018). Improving genetic transformation rates in honeybees. *Scientific Reports*, *8*(1), 16534. https://doi.org/10.1038/s41598-018-34724-w
Robertson, H. M. (2019). Molecular Evolution of the Major Arthropod Chemoreceptor Gene Families. *Annual Review of Entomology*, *64*(1), 227–242. https://doi.org/10.1146/annurev-ento-020117-043322

Robinson, G. E., Grozinger, C. M., & Whitfield, C. W. (2005). Sociogenomics: social life in molecular terms. *Nature Reviews. Genetics*, *6*(4), 257–270. https://doi.org/10.1038/nrg1575

Robinson, M. D., McCarthy, D. J., & Smyth, G. K. (2010). edgeR: a Bioconductor package for differential expression analysis of digital gene expression data. *Bioinformatics*, *26*(1), 139–140. https://doi.org/10.1093/bioinformatics/btp616

Rössler, W., Spaethe, J., & Groh, C. (2017). Pitfalls of using confocal-microscopy based automated quantification of synaptic complexes in honeybee mushroom bodies (response to Peng and Yang 2016). *Scientific Reports*, *7*(1), 9786. https://doi.org/10.1038/s41598-017-09967-8

Roth, A., Vleurinck, C., Netschitailo, O., Bauer, V., Otte, M., Kaftanoglu, O., … Beye, M. (2019). A genetic switch for worker nutrition-mediated traits in honeybees. *PLOS Biology*, *17*(3), e3000171. https://doi.org/10.1371/journal.pbio.3000171

Sato, K., Pellegrino, M., Nakagawa, T., Nakagawa, T., Vosshall, L. B., & Touhara, K. (2008). Insect olfactory receptors are heteromeric ligand-gated ion channels. *Nature*, *452*(7190), 1002–1006. https://doi.org/10.1038/nature06850

Schindelin, J., Arganda-Carreras, I., Frise, E., Kaynig, V., Longair, M., Pietzsch, T., … Cardona, A. (2012). Fiji: an open-source platform for biological-image analysis. *Nature Methods*, *9*(7), 676–682. https://doi.org/10.1038/nmeth.2019

Schmehl, D. R., Tomé, H. V. V, Mortensen, A. N., Martins, G. F., & Ellis, J. D. (2016). Protocol for the in vitro rearing of honey bee (Apis mellifera L.) workers. *Journal of Apicultural Research*, *55*(2), 113–129. https://doi.org/10.1080/00218839.2016.1203530

Schmuker, M., Yamagata, N., Nawrot, M. P., & Menzel, R. (2011). Parallel representation of stimulus identity and intensity in a dual pathway model inspired by the olfactory system of the honeybee. *Frontiers in Neuroengineering*. https://doi.org/10.3389/fneng.2011.00017

Schulte, C., Theilenberg, E., Müller-Borg, M., Gempe, T., & Beye, M. (2014). Highly efficient integration and expression of piggyBac-derived cassettes in the honeybee (Apis mellifera). *Proceedings of the National Academy of Sciences of the United States of America*, *111*(24), 9003–9008. https://doi.org/10.1073/pnas.1402341111

Shpigler, H. Y., Saul, M. C., Murdoch, E. E., Cash-Ahmed, A. C., Seward, C. H., Sloofman, L., … Robinson, G. E. (2017). Behavioral, transcriptomic and epigenetic responses to social challenge in honey bees. *Genes, Brain and Behavior*, *16*(6), 579–591. https://doi.org/10.1111/gbb.12379

Supek, F., Bošnjak, M., Škunca, N., & Šmuc, T. (2011). REVIGO Summarizes and Visualizes Long Lists of Gene Ontology Terms. *PLoS ONE*, *6*(7), e21800. https://doi.org/10.1371/journal.pone.0021800

Traniello, I. M., Bukhari, S. A., Kevill, J., Ahmed, A. C., Hamilton, A. R., Naeger, N. L., … Robinson, G. E. (2020). Meta-analysis of honey bee neurogenomic response links Deformed wing virus type A to precocious behavioral maturation. *Scientific Reports*, *10*(1), 1–12. https://doi.org/10.1038/s41598-020-59808-4

Trible, W., Olivos-Cisneros, L., McKenzie, S. K., Saragosti, J., Chang, N.-C., Matthews, B. J., … Kronauer, D. J. C. (2017). orco Mutagenesis Causes Loss of Antennal Lobe Glomeruli and Impaired Social Behavior in Ants. *Cell*, *170*(4), 727-735.e10. https://doi.org/10.1016/j.cell.2017.07.001

Wallberg, A., Bunikis, I., Pettersson, O. V., Mosbech, M. B., Childers, A. K., Evans, J. D., … Webster, M. T. (2019). A hybrid de novo genome assembly of the honeybee, Apis mellifera, with chromosome-length scaffolds. *BMC Genomics*, *20*(1), 275.

https://doi.org/10.1186/s12864-019-5642-0
Wanner, K. W., Nichols, A. S., Walden, K. K. O., Brockmann, A., Luetje, C. W., & Robertson, H. M. (2007). A honey bee odorant receptor for the queen substance 9-oxo-2-decenoic acid. *Proceedings of the National Academy of Sciences of the United States of America*, *104*(36), 14383–14388. https://doi.org/10.1073/pnas.0705459104
Wicher, D. (2018). Tuning insect odorant receptors. *Frontiers in Cellular Neuroscience*. https://doi.org/10.3389/fncel.2018.00094
Wicher, D., Schäfer, R., Bauernfeind, R., Stensmyr, M. C., Heller, R., Heinemann, S. H., & Hansson, B. S. (2008). Drosophila odorant receptors are both ligand-gated and cyclic-nucleotide- activated cation channels. *Nature*, *452*(7190), 1007–1011. https://doi.org/10.1038/nature06861
Winston, M. L., & Slessor, K. N. (1998). Honey bee primer pheromones and colony organization: gaps in our knowledge. *Apidologie*, *29*(1–2), 81–95. https://doi.org/10.1051/apido:19980105
Yamagata, N., Schmuker, M., Szyszka, P., Mizunami, M., & Menzel, R. (2009). Differential odor processing in two olfactory pathways in the honeybee. *Frontiers in Systems Neuroscience*. https://doi.org/10.3389/neuro.06.016.2009
Yan, H., Jafari, S., Pask, G., Zhou, X., Reinberg, D., & Desplan, C. (2020, February 1). Evolution, developmental expression and function of odorant receptors in insects. *The Journal of Experimental Biology*. NLM (Medline). https://doi.org/10.1242/jeb.208215
Yan, H., Opachaloemphan, C., Mancini, G., Yang, H., Gallitto, M., Mlejnek, J., … Desplan, C. (2017). An Engineered orco Mutation Produces Aberrant Social Behavior and Defective Neural Development in Ants. *Cell*, *170*(4), 736-747.e9. https://doi.org/10.1016/J.CELL.2017.06.051
Zhao, H., Du, Y., Gao, P., Wang, S., Pan, J., & Jiang, Y. (2016). Antennal transcriptome and differential expression analysis of five chemosensory gene families from the Asian honeybee Apis cerana cerana. *PLoS ONE*. https://doi.org/10.1371/journal.pone.0165374
Zhou, X., Rokas, A., Berger, S. L., Liebig, J., Ray, A., & Zwiebel, L. J. (2015). Chemoreceptor evolution in Hymenoptera and its implications for the evolution of eusociality. *Genome Biology and Evolution*. https://doi.org/10.1093/gbe/evv149
Zhou, X., Slone, J. D., Rokas, A., Berger, S. L., Liebig, J., Ray, A., … Zwiebel, L. J. (2012). Phylogenetic and Transcriptomic Analysis of Chemosensory Receptors in a Pair of Divergent Ant Species Reveals Sex-Specific Signatures of Odor Coding. *PLoS Genetics*, *8*(8), e1002930. https://doi.org/10.1371/journal.pgen.1002930